tissue) were incubated with 0.12 nM [^{3}H]QNB (46 Ci/mmol, Amersham) alone or in the presence of test compound in a total volume of 5 mL for 30 min at 37 °C. The reaction was stopped by adding 5 mL of ice-cold buffer and rapid filtration through Whatman GF/B filters soaked previously in 0.1% polyethylenimine (Sigma) for a minimum of 30min. The filters were washed twice with the same volume of buffer and bound radioactivity estimated by liquid scintillation counting methods. Each compound was tested in five different concentrations, and nonspecific binding estimated at 20 μM atropine. All estimations were made in triplicate, and each displacement experiment was repeated at least twice. The dissociation constant (K_d) for the binding of [^{3}H]QNB to rat brain membranes was determined to 13.7 ± 0.9 pM based on Scatchard analysis following a previously described procedure.[17]

The procedure for determinations of inhibition of [^{3}H]QNB binding to rat heart tissue was the same as that described above with the exceptions that the tissue was homogenized in an ultraturrax homogenizer and that 4 mg of tissue was used per assay. A Scatchard analysis of [^{3}H]QNB binding to rat heart tissue gave a K_d value of 9.1 ± 0.7 pM.

The procedure for the determinations of inhibition of [^{3}H]PZ binding to rat brain membranes was analogous to that described above for [^{3}H]QNB binding to such membrane fractions: 3 mg of tissue were incubated with 1.0 nM [^{3}H]PZ (85 Ci/mmol, New England Nuclear) at 25 °C for 60 min in a total volume of 1.5 mL of buffer. The reaction was stopped by filtration under reduced pressure followed by three washes with 4 mL of ice-cold buffer. Nonspecific binding was estimated at 10 μM atropine. A K_d value of 1.8 ± 1.0 nM for the binding of [^{3}H]PZ to rat brain membranes was derived from a Scatchard analysis.

The procedure for determination of inhibition of [^{3}H]Oxo-M binding to rat brain membranes was analogous to that described above for [^{3}H]QNB binding to such membrane fractions: 5 mg of tissue were incubated with 0.2 nM [^{3}H]Oxo-M (84.4 Ci/mmol, New England Nuclear) at 30 °C for 40 min in a total volume of 1.5 mL of buffer. The reaction was stopped by adding 5 mL of ice-cold buffer, rapid filtration, and one wash with the same volume of buffer. A K_d value of 0.48 ± 0.03 nM for the binding of [^{3}H]Oxo-M to rat brain membranes was derived from a Scatchard analysis.

Acknowledgment. This work was supported by grants from the Danish Medical and Technical Research Councils. The secretarial assistance of B. Hare and the technical assistance of T. Lindgreen and S. Stilling are gratefully acknowledged. The gifts of sulfoarecoline and sulfoarecaidine ethyl ester from Dr. U. Moser and Professor G. Lambrecht, Johann Wolfgang Goethe-Universität, Frankfurt/Main, West Germany, are cordially acknowledged.

Registry No. 1, 1198-44-3; 2, 113748-37-1; 3, 113748-38-2; 4, 113748-39-3; 5a, 113748-40-6; 5b, 113748-45-1; 5c, 113748-46-2; 5d, 113748-47-3; 6a, 113748-41-7; 7a, 113748-42-8; 7b, 113748-48-4; 7c, 113748-49-5; 7d, 113748-50-8; 8a, 113748-43-9; 9, 113748-44-0; 0,5-dimethyl-THPO·HCl, 95597-35-6; C_2H_5Br, 74-96-4; $(CH_3)_2CHBr$, 75-26-3; $HC{\equiv}CCH_2Br$, 624-65-7.

2,3-Diarylindenes and 2,3-Diarylindenones: Synthesis, Molecular Structure, Photochemistry, Estrogen Receptor Binding Affinity, and Comparisons with Related Triarylethylenes

Gregory M. Anstead, Robert J. Altenbach, Scott R. Wilson, and John A. Katzenellenbogen*

Department of Chemistry, University of Illinois, Urbana, Illinois 61801. *Received December 7, 1987*

Two 2,3-diphenylindene and -indenone systems, with potential fluorescent and photofluorogenic properties, were prepared and studied as ligands for the estrogen receptor. The indene systems were prepared by Friedel–Crafts cyclization of appropriate α-benzyl desoxybenzoin systems, and the indenones either by oxidation of the indenes, by cyclization of α-benzoyl desoxybenzoins, or by acylium ion attack on tolan. Crystallographic analysis of the 2,3-diphenylindene and -indenone systems shows the phenyl substituents twisted out of the plane of the indene/indenone systems, with both torsional angles greater in the indenone than indene system; the phenyl attachment to the five-membered ring allows these systems to be considerably more planar than the related 1,2-diphenyl-3,4-dihydronaphthalene and the triarylethylene nonsteroidal estrogens. In contrast to the diphenyldihydronaphthalenes, the diarylindene and -indenone systems undergo photocyclization to phenanthrenes inefficiently. The estrogen receptor binding affinity of these systems is reasonably high (9–59% relative to estradiol), with the indenone systems having higher affinity than the indenes; additional hydroxyl substitution raises the affinity of the indenes but lowers that of the indenones. These trends can be rationalized by considering differences in molecular volumes or surface areas (related to torsional angles) and specific polar interactions.

Two nafoxidine[1] analogues of high estrogen receptor (ER) binding affinity, **1** and **2**, have been described as photofluorogenic estrogens.[2,3] In these compounds, the *cis*-stilbene unit of the diaryldihydronaphthalene is photochemically converted to a fluorescent phenanthrenoid.[4] Such ER-targetted fluorophores have been proposed to quantitate the ER in individual cells, thereby providing a clinically useful prognostic technique in the management of breast cancer.[5]

The 2,3-diarylindenes (**3**)[6] were originally envisaged as another class of photofluorogenic estrogens. However, deletion of one methylene unit from the dihydronaphthalene caused dramatic changes in the ER binding affinity and in the photochemical and fluorescence properties. In addition, 2,3-diarylindenones (**4**) result from

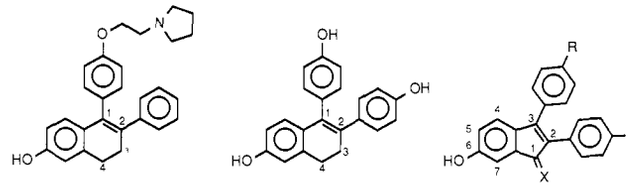

1 **2** **3** (X=H_2): a, R=H; b, R=OH. **4** (X=O): a, R=H; b, R=OH.

* Address correspondence to John A. Katzenellenbogen, 461 Roger Adams Laboratory, Box 37, 1209 W. California St., University of Illinois, Urbana, IL 61801.

(1) Duncan, G. W.; Lyster, S. C.; Clark, J. J.; Lednicer, D. *Proc. Soc. Exp. Biol. Med.* **1963**, *112*, 439.
(2) Bindal, R. D.; Katzenellenbogen, J. A. *J. Steroid Biochem.* **1985**, *23*, 929.

0022-2623/88/1831-1316$01.50/0

Scheme I

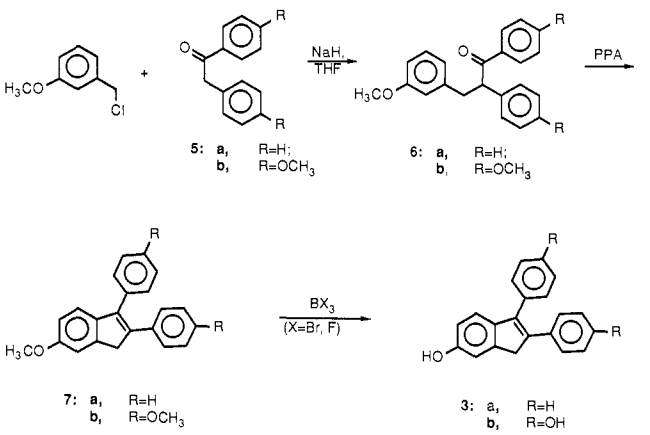

facile air oxidation of the indenes; these compounds are nonfluorescent and nonphotofluorogenic but have higher ER binding affinity than the corresponding indenes.

In this paper, we address the common structural basis for the fluorescence and photocyclization properties and the ER binding affinity of the diarylindenes and diarylindenones.

Results and Discussion

Chemical Syntheses. Our route to the indenes was similar to that of Crenshaw[7] but with methodological improvements (Scheme I). The indenones rapidly formed in small quantities when the indenes were dissolved in air-exposed solvents. However, an efficient, general method for the direct conversion of the indenes to the indenones proved elusive. Traditional allylic oxidants, such as CrO_3,[8] SeO_2,[9] and dichlorodicyanobenzoquinone,[10] employed under a variety of conditions, gave low and variable yields of the indenones.

A modification of Scheme I was used to prepare the indenones (Scheme II). Active ester **8** gave modest yields of diketones **9a** and **9b**, due to the difficulty in removing the 4-nitrophenol byproduct. The acid chloride of 3-methoxybenzoic acid has recently become commercially available[11] and is probably a more effective acylating agent.[12]

Cyclodehydration of methoxy diketone **9a** to the desired indenone **10a** was effected by $MeSO_3H$.[13] In contrast to the indene cyclization, the product of cyclization ortho to

Scheme II

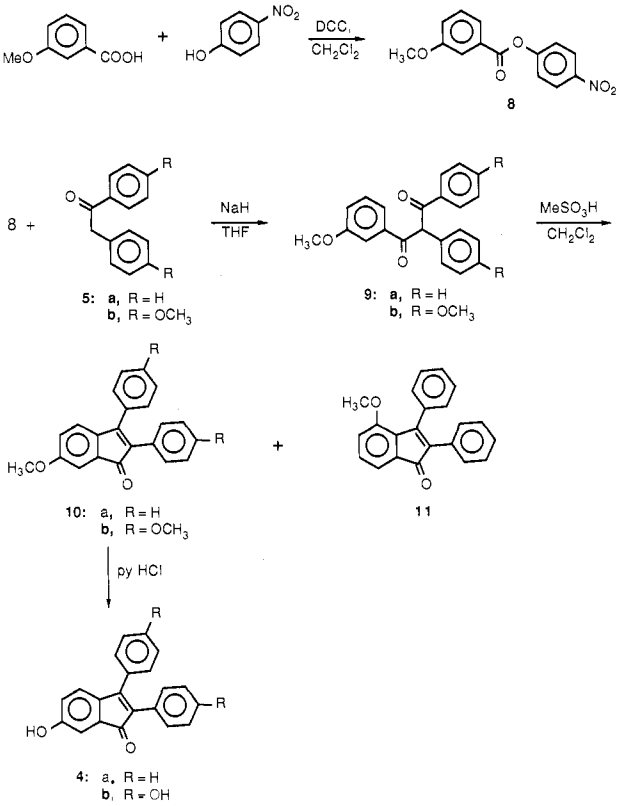

Scheme III

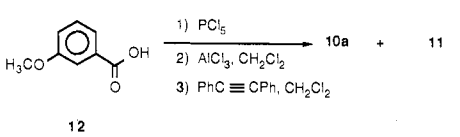

the methoxy group (**11**) was also formed: at 25 °C, the ratio of **10a** to **11** was 9:1, with an isolated yield of **10a** of 62%; at 0 °C, the **10a**/**11** ratio increased to 16.4:1, with 80% of **10a** isolated; no reaction occurred at −30 °C. The typical cyclodehydration conditions (PPA) as used in Scheme I gave lower ratios of **10a**/**11**. The less electrophilic trimethoxy diketone **9b** gave solely the para isomer **10b**, even at 25 °C. Boron trifluoride[14] and trimethylsilyl iodide[15] were incompatible with the enone system, so pyridine hydrochloride[16] was used as the deprotection reagent.

An alternate one-pot approach to indenone **10a** was based on the work of Martens and Hoornaert[17] (Scheme III). In situ generation of the acid chloride from acid **12** and subsequent addition of $AlCl_3$ formed the acylium ion, which was trapped by tolan to give a vinyl cation. This cation cyclized to give indenones **10a** and **11**. Unfortunately, the regioselectivity of this cyclization was consistently poor (**10a**/**11** ≈ 2), due to the high reactivity of the vinyl cation. This route was abandoned in favor of that shown in Scheme II.

Molecular Structures. Crystallographic structure determinations were performed on trimethoxyindene **7b** and methoxyindenone **10a**. Two perspectives on these molecules are shown in Figure 1. Introduction of a carbonyl at C-1 increases the torsional angles of the planes

(3) Bindal, R. D.; Katzenellenbogen, J. A. *Photochem. Photobiol.* **1986**, *43*, 121.
(4) Mallory, F. B.; Mallory, C. W. *Org. React. (N.Y.)* **1984**, *30*, 1.
(5) Fevig, T. L.; Lloyd, J. E.; Zablocki, J. A.; Katzenellenbogen, J. A. *J. Med. Chem.* **1987**, *30*, 156 and references cited therein.
(6) Lednicer, D.; Babcock, J. C.; Marlatt, P. E.; Lyster, S. C.; Duncan, G. W. *J. Med. Chem.* **1965**, *8*, 52.
(7) Crenshaw, R. R.; Jenks, T. A.; Baily, G. *J. Med. Chem.* **1974**, *17*, 1127.
(8) Garza, G. A.; Rao, P. N. *Steroids* **1983**, *42*, 3188.
(9) Bhalerao, V. T.; Rapoport, H. *J. Am. Chem. Soc.* **1971**, *93*, 4835.
(10) Lee, H.; Harvey, R. G. *J. Org. Chem.* **1983**, *48*, 749.
(11) Aldrich Catalog Handbook of Fine Chemicals, 1986.
(12) For other benzyl ketones, we have found that 3-methoxybenzoyl chloride provides a higher yield of the dione than the PNP ester does for the deoxybenzoin systems (Anstead, G. M.; Ensign, J. L.; Wilson, S. R.; Katzenellenbogen, J. A., manuscript in preparation, 1988). For a discussion of the use of acid chlorides as acylating agents for ketones, see: House, H. O.; Auerbach, R. A.; Gall, M.; Peet, N. P. *J. Org. Chem.* **1973**, *38*, 514.
(13) Leon, A. A.; Daub, G.; Silverman, I. R. *J. Org. Chem.* **1984**, *49*, 4544.
(14) Williard, P. G.; Fryhle, C. B. *Tetrahedron Lett.* **1980**, *21*, 3731.
(15) Jung, M. E.; Lyster, M. A. *J. Org. Chem.* **1977**, *42*, 3761.
(16) Sheehan, J. C.; Erman, W. F.; Cruickshank, P. A. *J. Am. Chem. Soc.* **1957**, *79*, 147.
(17) Martens, H.; Hoornaert, G. *Synth. Commun.* **1972**, *2*, 147.

Table I. Olefinic Bond Angles in **7b**, **10a**, **13**, and **14**

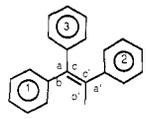

bond angle	7b	10a	13[a]	14A[b]
a	121.6°	121.1°	116.6°	113.8°
b	108.9°	110.4°	120.8°	122.6°
c	129.5°	128.2°	122.5°	123.6°
a′	119.7°	123.5°	115.4°	115.3°
b′	109.9°	107.7°	118.9°	122.5°
c′	130.4°	128.8°	125.7°	122.2°
total of deviations from 120°	43.0°	43.5°	16.7°	21.8°

[a] Reference 23. [b] Reference 24.

of the three aromatic rings with respect to the double bond. The carbonyl group increases the torsion angles of both pendant aryl groups by the same magnitude, suggesting that ring rotation is correlated in the 2,3-diarylindene/indenone systems. Correlated rotation has been noted in the related tetraarylcyclopentadienone system.[18]

Indenone **10a** had no intermolecular contacts less than the sum of van der Waals radii, so the observed solid-state structure is at or near a local minimum energy conformation. The crystal structure of 2,3-diphenylindenone[19] is very similar to that of **10a**; the aryl double bond dihedral angles differ by less than 6°. Perhaps these minor differences can be accounted for by weak crystal packing forces imposed on a relatively broad energy minima for aryl rotation.[20] Indene **7b** had two intermolecular hydrogen–oxygen contacts less than the sum of van der Waals radii, but neither contact involved hydrogen atoms on the pendant aryl groups and both contacts exceeded 2.5 Å. The observed indene structure, with the possible exception of methoxy rotation, is also at or near a local minimum energy conformation. The observed conformations of **7b** and **10a** probably represent global energy minima, because there is only one unique molecule per asymmetric unit[21] and the intermolecular forces in each case are minimal.

Neither indene **7b** nor indenone **10a** have the characteristic propeller conformation of typical triarylethylenes.[22] The five-membered ring constrains the fused phenyl to approximate coplanarity with the double bond and splays the pendant rings apart, allowing the reduction in the aryl double torsional angles. The distortion of the usual olefinic bond angles is shown in Table I and is greater than that in tamoxifen (**13**)[23] and nafoxidine (**14**).[24]

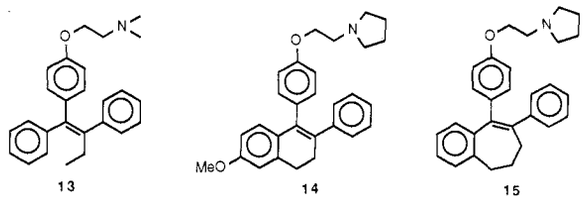

13 14 15

Scheme IV

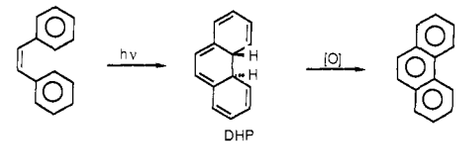

DHP

Scheme V

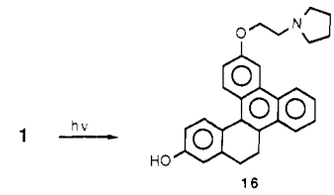

16

Scheme VI

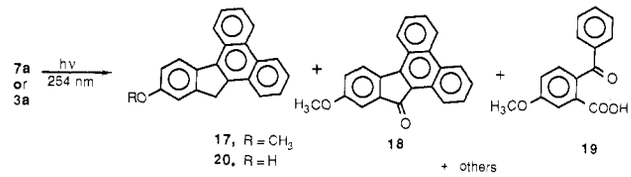

17, R = CH_3
20, R = H
18
19
+ others

Overall, indene **7b** and indenone **10a** are more planar than other triarylethylene ER ligands that have been analyzed crystallographically: tamoxifen (**13**),[23] nafoxidine (**14**),[24] and homonafoxidine (**15**).[25] A comparison of the three prominent torsional angles among the triarylethylenes mentioned herein is made in Table II.

UV Spectra. Differences in molecular structure between indene **7a**, tamoxifen (**13**), nafoxidine (**14**), and indenone **4a** are also apparent from the UV spectra (Table III). Compared to 4-methoxy-*trans*-stilbene, diarylindene **7a** shows a slight red shift in the lowest energy absorbance band and a modest hypochromic effect. Nafoxidine also shows absorbance above 300 nm, like 4-methoxy-*trans*-stilbene, but at a shorter wavelength with marked hypochromicity. Thus, as the torsional angle of the 2-aryl substituent increases, the longest wavelength *trans*-stilbene band decreases in intensity. The spectrum of tamoxifen is similar to that of 4-methoxy-*cis*-stilbene, consistent with the large torsional angles of all three aryl groups and the consequent complete loss of the lowest energy methoxy-*trans*-stilbene chromophore. Indenone **4a** shows loss of the *trans*-stilbenoid band at about 310 nm and has a low intensity, long wavelength band ascribed to a $\pi \rightarrow \pi^*$ transition in simpler indenones.[27]

Photochemistry. The *cis*-stilbene photocyclization proceeds by conrotation in the S_1 state to give a dihydrophenanthrene (DHP) intermediate, which undergoes oxidation to the phenanthrene (Scheme IV).[4] In like manner, hydroxynafoxidine (**1**) is photochemically converted into phenanthrene **16** rapidly (<30 min) and efficiently (>82% yield) (see Scheme V).[2] However, compound **7a**, an indene congener of **1**, behaved much differently; under a number of experimental conditions (Table IV), the yields of the expected phenanthrene **17**

(18) Haywood-Farmer, J.; Battiste, M. A. *Chem. Ind. (London)* **1971**, 1232.
(19) Jens, K.-J.; Weiss, E. *Chem. Ber.* **1984**, *117*, 2469.
(20) Kuroda, R.; Cutbush, S.; Neidle, S.; Leung, O.-T. *J. Med. Chem.* **1985**, *28*, 1497.
(21) Duax, W. L.; Griffin, J. F.; Weeks, C. M.; Korach, K. S. *Environ. Health Perspect.* **1985**, *61*, 111.
(22) Gilbert, J.; Miquel, J.-F.; Précigoux, G.; Hospital, M.; Raynaud, J.-P.; Michel, F.; Crastes de Paulet, A. *J. Med. Chem.* **1983**, *26*, 693.
(23) Précigoux, G.; Courseille, C.; Goeffre, S.; Hospital, M. *Acta Crystallogr., Sect. B.: Struct. Crystallogr. Cryst. Chem.* **1979**, *B35*, 3070.
(24) Camerman, N.; Chan, L. Y. Y.; Camerman, A. *J. Med. Chem.* **1980**, *23*, 941.
(25) McCague, R.; Kuroda, R.; Leclerq, G.; Stoessel, S. *J. Med. Chem.* **1986**, *29*, 2053.
(26) Précigoux, G.; Leroy, F.; Hospital, M. *Cryst. Struct. Commun.* **1981**, *10*, 647.
(27) Kuboyama, A.; Matsumoto, H. *Bull. Chem. Soc. Jpn.* **1979**, *52*, 1796.
(28) Shari, T.; Gazit, A.; Livshitz, T.; Biran, S. *J. Med. Chem.* **1985**, *28*, 1504.

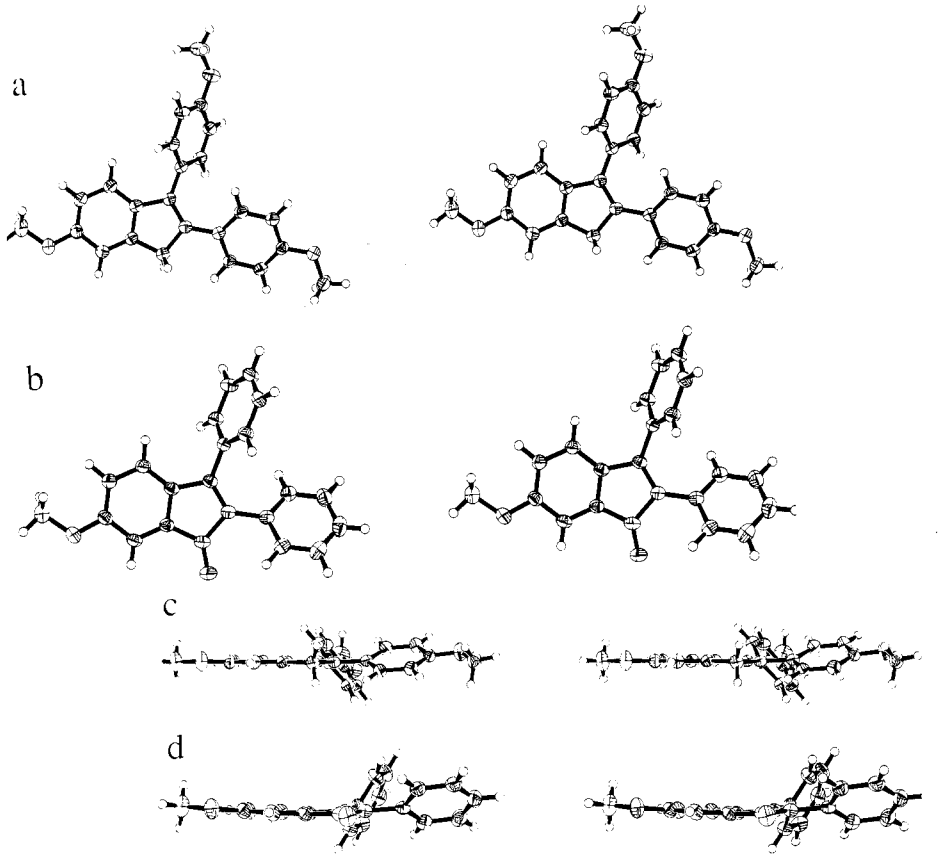

Figure 1. Stereoscopic thermal ellipsoid representations: (a) and (b), **7b** and **10a** plotted parallel to the best-plane normal, respectively; (c) and (d), **7b** and **10a** plotted perpendicular to the best-plane normal, respectively.

Table II. Torsional Angles (deg) between Prominent Planes in Triarylethylenes

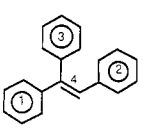

torsion angle	indene **7b**	indenone **10a**	2,3-diphenyl-indenone[a]	tamoxifen (**13**)[b]	nafoxidine (14) A[c]	nafoxidine (14) B[d,e]	nafoxidine (14) C[f]	homonafoxidine (**15**)[d,e]
1–4	1	5	4	64	20	19	17	45
2–4	27	34	37	57	50	44	45	45
3–4	49	55	49	50	56	69	61	53
total[g] torsion	77	94	90	172	126	132	123	143

[a] Reference 19. [b] Reference 23. [c] Reference 24. [d] Crystallography performed on analogue without basic ether side chain. [e] Reference 25. [f] Reference 26. [g] Sum of the three prominent torsional angles.

Table III. UV Spectral Data of Selected Triarylethylenes and Related Compounds

compound	λ_{max}, nm (ϵ)
4-methoxy-*cis*-stilbene[a,b]	280 (10 600)
4-methoxy-*trans*-stilbene[a,b]	306 (29 000), 310 (27 500)
indene **7a**[c]	236 (28 200), 316 (22 500)
tamoxifen (**13**)[a,b]	238 (16 200), 277 (10 650), 288 (10 400)
nafoxidine (14)[c,d]	258 (11 000), 304 (13 000)
indenone **4a**[c]	272 (36 100), 498 (1380)

[a] 95% EtOH. [b] Reference 28. [c] EtOH. [d] Reference 2.

were low, and complex product mixtures resulted (Scheme VI). Phenolic indene **3a** also gave a low yield of the desired phenanthrene **20** (Scheme VI). Thus, the photocyclization of the indenes[29] was quite sluggish and inefficient compared to the dihydronaphthalene systems.[2,3] Little photocyclization was previously observed for 2,3-diphenylindenone.[30]

Considerations of molecular geometry may explain the differences in photochemical behavior between the indenes and dihydrophenanthrenes. The greater planarity of the diarylindene as compared to the diaryldihydrophenanthrene may have several consequences, all of which attenuate the propensity to photocyclize: (1) the distance and/or orientation of the appropriate ortho carbons is not optimal, (2) the less flexible indene is unable to assume the proper transition state geometry (a skewed DHP),[4] and (3) fluorescence emission becomes an available deactivation pathway. Fluorescence emission from indene **7a** is appreciable (Φ_F = 0.15 in ethanol), whereas fluorescence from **1** or **2** is difficult to measure due to the rapid photocyclization. Competition between deactivation processes

(29) For a discussion of the photocyclization of compounds related to 2,3-diarylindenes, see: Padwa, A.; Goldstein, S.; Loza, R.; Pulwer, M. *J. Org. Chem.* **1981**, *46*, 1858.

(30) A photochemical precursor to 2,3-diphenylindenone was reported to give only trace amounts of a cyclized material upon irradiation; see: Harspool, W. M. *J. Chem. Soc., Chem. Commun.* **1969**, 467.

Table IV. Conditions and Results of Irradiation of **7a**[a,b]

trial	degas?	atmosphere	equiv I_2	time, h	recovered **7a**	yields, %		
						17	**18**	**19**
1	no	N_2	0.05	2.5	82	11	nil	*d*
2	yes	N_2	0.56	14.5	small[c]	24	*d*	*d*
3	yes	N_2	0.05	10.5	small[c]	*d*	32	*d*
4	yes	N_2	0.06	9.5	nil	10	6	*d*
5	no	air	nil	4	nil	5	18	11
6	no	air	nil	13	small[c]	*d*	3	10

[a] All used cyclohexane as solvent except trial 1, which used 4:1 MeOH–benzene. [b] All used concentrations of **7a** of 0.02 M except 1, which used 0.016 M. [c] Less than 2%, contaminated with small amounts of impurities. [d] Observed by TLC but not isolated.

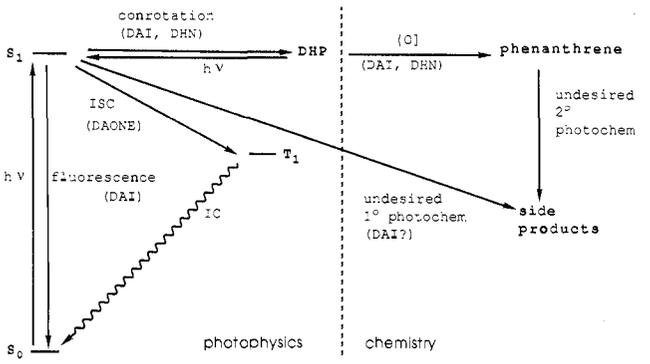

Figure 2. Summary of the chemical and photophysical behavior of the 2,3-diarylindenes (DAI), 1,2-diaryldihydronaphthalenes (e.g., 1; DHN), and 2,3-diarylindenones (DAONE). ISC refers to intersystem crossing; IC refers to internal conversion.

of electronically excited stilbenes is well-documented.[31] The indenones do not photocyclize or fluoresce appreciably because the cross-conjugated carbonyl induces intersystem crossing, thereby deenergizing S_1. The chemical and photophysical behavior of the indenes, dihydronaphthalenes, and indenones is summarized in Figure 2. With fluorescence decreasing the rate of formation of the DHP from the S_1 state of the diarylindene, undesired secondary photochemical processes decrease the yield of the phenanthrene.

Clinically the triarylethylenes have phototoxic side effects,[32] and there have been efforts to develop triarylethylene analogues to circumvent this problem.[33] The stilbene photocyclization may be implicated in this toxicity because it generates a phenanthrene of considerably different topology that may not be accommodated by metabolizing enzymes[34] or that may be metabolically activated to toxic diol epoxides.[35]

The diarylindenes and -indenones, with less propensity to photocyclize, may be less phototoxic. Although enones, in general, are photoreactive and have been used as photoaffinity labels,[36] as aromatic substitution increases and electron-rich groups are added, the reactivity is mollified.[37] We have tried to photoinactivate the ER[38] with indenones

Table V. Estrogen Receptor Binding Affinities[a]

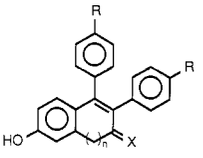

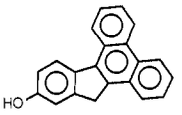

20

compd	*n*	X	R	RBA,[b] %
3a	0	H_2	H	8.9
3b	0	H_2	OH	15
4a	0	O	H	59
4b	0	O	OH	23
2	1	H_2	OH	140
20				0.01

[a] Determined by competitive radiometric binding assay with rat uterine cytosol as a source of receptor, [^{3}H]estradiol as tracer, and dextran-coated charcoal as absorbant for free ligand. For details, see ref 39. [b] Binding affinities are expressed relative to that of estradiol = 100% (RBA = relative binding affinity) and are the average of duplicate determinations. These measurements are generally reproducible to ±30%.

4a and **4b** and 2,3-diphenylindenone, but no specific photoinactivation occurred (data not shown).

Structure–Receptor Binding Affinity Relationships. The ER binding affinities (RBA) were determined by using a competitive protein binding assay[39] (see Table V). Large differences in RBA are evident for three pairs of congeners. The phenanthrene **20** has an affinity 1000 times less than the corresponding indene **3a**. Dihydronaphthalene **2** has an affinity 10 times that of its triphenolic indene counterpart **3b**. Monophenolic indenone **4a** has a sevenfold greater affinity than monophenolic indene **3a**.

A modest enhancement in RBA was found for triphenol indene **3b** compared to its analogous monophenol **3a**. This may be due to additional hydrogen-bonding interactions in the ER binding site and will be treated in a future publication.[40] Conversely, triphenol indenone **4b** has a lower RBA than monophenol indenone **4a**. Since the C-1 carbonyl increases the RBA in both of the cases studied (**4a** vs **3a**; **4b** vs **3b**), this indicates that the RBA enchancement effects of carbonyl and *p*-hydroxy substitution are not additive. Perhaps the overall polarity of triphenolic indenone **4b** is what limits its RBA.

McCague et al.[25] have recently described the dihedral angle effects on the RBA of certain triarylethylenes. Nafoxidine (**14**), with smaller torsional angles, has a lower RBA than **13** or **15**, which have more comparable torsion (see Table II, bottom line). The torsional angles of the

(31) (a) Wismonski-Knittel, T.; Fischer, E. *J. Chem. Soc., Perkin Trans. II* **1979**, 449. (b) Wismonski-Knittel, T.; Fischer, G.; Fischer, E. *J. Chem. Soc., Perkin Trans. II* **1974**, 1930.
(32) Legha, S. S.; Slavik, M.; Carter, S. K. *Cancer* **1976**, *38*, 1535.
(33) Katzenellenbogen, J. A.; Katzenellenbogen, B. S.; Tatee, T.; Robertson, D. W.; Landvatter, S. W. In *Estrogens in the Environment*; McLachlan, J. A., Ed.; Elsevier North Holland: Amsterdam, 1980; Vol. 1, pp 33–51.
(34) For a discussion of the metabolism of tamoxifen, see: Jordan, V. C. *Pharmacol. Rev.* **1984**, *36*, 245.
(35) Harvey, R. G. *Acc. Chem. Res.* **1981**, *14*, 218.
(36) Katzenellenbogen, J. A.; Katzenellenbogen, B. S. *Vitam. Horm. (N.Y.)* **1984**, *41*, 213.
(37) Bayley, H. *Photogenerated Reagents in Biochemistry and Molecular Biology*; Elsevier: Amsterdam, 1983.
(38) Katzenellenbogen, J. A.; Johnson, H. J., Jr.; Carlson, K. E.; Myers, H. N. *Biochemistry* **1974**, *13*, 2986.
(39) Katzenellenbogen, J. A.; Johnson, H. J., Jr.; Myers, H. N. *Biochemistry* **1973**, *12*, 4085.
(40) Anstead, G. M.; Peterson, C. S.; Katzenellenbogen, J. A., manuscript in preparation.

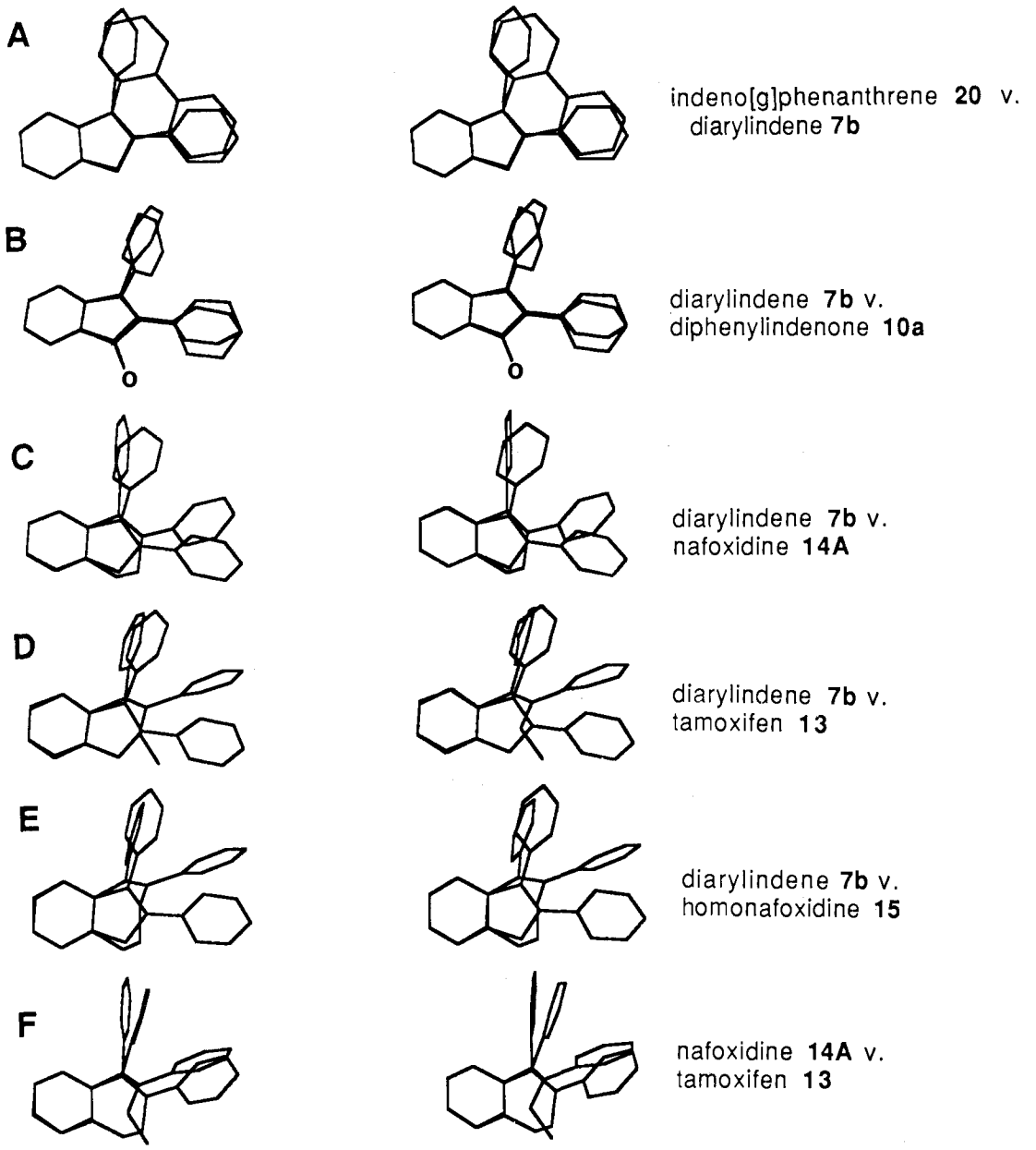

Figure 3. Stereoview of the overlap of 1-ring (designation from Table II) of various triarylethylenes. The geometry of **20** was determined by molecular mechanics; other structures were determined by crystallography. Only carbon skeletons are shown for clarity, except for **10a**, where the carbonyl oxygen is also shown.

Table VI. Comparisons of Triarylethylenes in Spatial Orientation of Molecular Features[a]

structural feature	distance (Å) between corresponding structure features in Figure 3: A	B	C	D	E	F
proximal double bond carbon[b]	0.037	0.210	0.300	0.336	0.326	0.143
distal double bond carbon[c]	0.070	0.265	0.934	1.706	1.355	0.828
3–3′[d]	0.579	0.750	0.822	2.331	1.833	2.112
2–2′[d]	0.442	0.558	2.234	2.997	2.500	0.833

[a] For comparison of relative spatial orientations, the 1-ring (cf. Table II for ring designations) of pairs of molecules were overlapped and the distances between the corresponding structural features were measured in angstroms. Overlap and measurement were done with the SYBYL molecular modeling program. [b] Double bond carbon closest to 1-ring. [c] Double bond carbon further from 1-ring. [d] The distance was measured from the centroids of the rings.

three aryl rings with respect to the double bond may affect the molecular volume and/or surface area. Similarly, in the indeno[*g*]phenanthrene (**20**),[41] diarylindene (**3a**), diarylindenone (**4a**) series, as the total torsion goes from 7° to 77° to 94°, the RBA increases from 0.01% to 9% to 59%. The more planar triphenol indene **3b** has a 10-fold lower affinity than its bulkier triphenol dihydronaphthalene analogue **2**.

However, another factor besides torsion needs to be considered in structure–RBA relationships among triarylethylenes. Introduction of bridging between the ethylene and the 1-ring changes not only the torsional angles but also the relative positions of the rings and ethylene carbons in space. The ring and double-bond positions in the triarylethylenes can be compared by

(41) The geometry of **20** was obtained from molecular mechanics calculations.

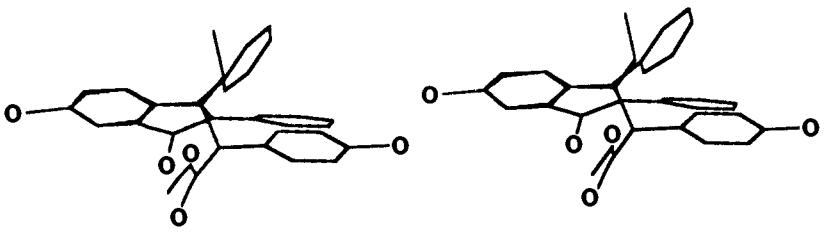

Figure 4. Stereoview of the superposition of the C-3 phenol of norhexestrol ester **21a** with the phenol of indenone **4a**. The conformation of **21a** was determined by molecular mechanics, with the preferred antiperiplanar conformation of *meso*-hexestrol as the initial geometry.[45] The structure of **4a** was determined by crystallography. Hydrogens have been omitted for clarity.

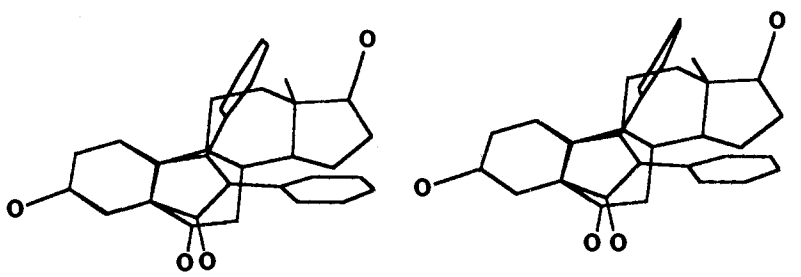

Figure 5. Stereoview of the superposition of the phenol of indenone **4a** with the A-ring phenol of 6-oxoestradiol (**23**). The structure of **23** was obtained by molecular mechanics, with the crystal structure of estradiol[47] as the initial geometry. The structure of the indenone was determined by crystallography.

overlapping the 1-ring and measuring the intermolecular distance between corresponding structural features. These overlaps appear in Figure 3 and the distances are recorded in Table VI.

The comparison of indene **7b** with indeno[*g*]-phenanthrene (**20**) indicates relatively little spatial difference in the molecular features described in Table VI. The RBA difference can therefore be directly related to the double bond–ring torsion changing the molecular profile. However, in the comparison of C–F of Figure 3, there are large distances between the molecular features, equivalent in some cases to about two carbon–carbon single bond lengths.[42] In these cases, the differences in RBA may be the combined result of both spatial and torsional effects.

The spatial differences between the molecular features of the indene and indenone are relatively small, and the torsional difference is also not very great (Figure 3, Table VI). It is possible these factors act synergistically. But, the indenones **4a** and **4b** also present the additional possibility of a polar interaction of the carbonyl with the ER, contributing to the RBA.

Specific polar interactions in the ER binding site have been invoked to explain the high RBA and stereospecificity of certain polar hexestrol analogues, **21**[43] and **22**.[43,44]

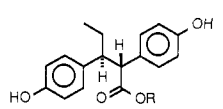

21a, R = CH_3
b, R = nC_5H_{11}

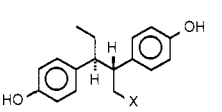

22a, X = F[44]
b, X = OH[43]

However, superposition of one of these compounds, **21a**, upon the indenone **4a** (Figure 4) showed that there are sizeable distances between the carbonyl oxygens, the carbonyl carbons, and the ester oxygen–carbonyl oxygen

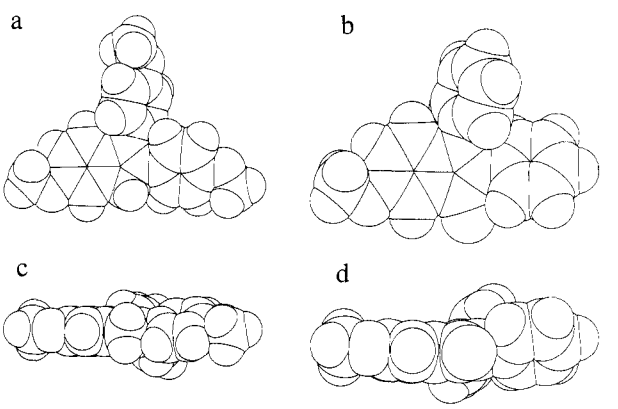

Figure 6. Space-filling representations: (a) and (b), **7b** and **10a** parallel to the best-plane normal, respectively; (c) and (d), **7b** and **10b** perpendicular to the best-plane normal, respectively.

(4.3, 3.6, and 5.6 Å, respectively). This suggests these two polar moieties do not interact with the same site in the ER, unless there is considerable receptor flexibility in this region or bridging via a water molecule.

The high RBA of indenone **4a** is surprising, considering the significantly lower RBA of 6-oxoestradiol (**23**) (20%).[46] If the fused phenol of the indenone is overlapped with the A-ring phenol of the steroid (see Figure 5), the carbonyl oxygens are only 0.58 Å apart. However, the electronic structure of the indenone carbonyl is different from a normal carbonyl. The typical dipolar resonance structure of a ketone (C^+–O^-) is stabilized in aryl ketone **23**, but this

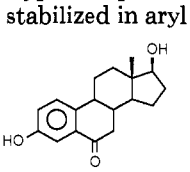

23

resonance form would represent an unstable antiaromatic system in an indenone.[48] Thus, although the carbonyls

(42) Table of Interatomic Distances and Configurations in Molecules and Ions *Spec. Publ.—Chem. Soc.* 1958, *No. 11.*
(43) Landvatter, S. W.; Katzenellenbogen, J. A. *Mol. Pharmacol.* **1981**, *20*, 43.
(44) Landvatter, S. W.; Katzenellenbogen, J. A. *J. Med. Chem.* **1982**, *25*, 1300.
(45) Kilbourn, M. R.; Arduengo, A. J.; Park, J. T.; Katzenellenbogen, J. A. *Mol. Pharmacol.* **1981**, *10*, 388.
(46) Katzenellenbogen, J. A. *Fed. Proc., Fed. Am. Soc. Exp. Biol.* **1978**, *37*, 174.
(47) Duax, W. L. *Acta Crystallogr., Sect. B.: Struct. Crystallogr. Cryst. Chem.* **1972**, *B28*, 1864.

are similarly disposed spatially in **4a** and **23**, the indenone carbonyl is less polar in character. Therefore, we still ascribe the higher RBA of indenone **4a** compared to its indene congener **3a** to its less planar molecular profile.

Gilbert et al.[22] have proposed that the inhibition of prostaglandin synthetase by triarylethylenes is governed by the accessibility of the 2-ring. If this is correct, indenes **7a,b** and indenones **10a,b** and **11** are excellent candidates as inhibitors of this enzyme since the geometry of these systems allows ample access to the 2-ring. Space-filling representations of **7b** and **10a** are shown in Figure 6.

Conclusions

The diarylindenes and -indenones have a more planar and compact structure than the triarylethylene antiestrogens nafoxidine and tamoxifen, resulting in some reduction in the estrogen receptor binding affinity. Due to the inefficient photocyclization, neither the indenes nor indenones are useful as photofluorogenic ligands. However, the fluorescent indenes may serve as the basis of an improved integrated fluorescent estrogen receptor ligand (Anstead, G. M.; Katzenellenbogen, J. A., manuscript in preparation). The diarylindenones are moderate-affinity ER ligands which, unlike tamoxifen, are resistant to isomerization during bioassay[49] and do not require stereospecific synthesis or the separation of *E* and *Z* isomers. With optimal hydroxyl substitution and/or the addition of a basic ether side chain, the diarylindenones may serve as high-affinity antiestrogens. On the basis of the structure–RBA relationships proposed herein, the design and synthesis of higher affinity diarylindenes and -indenones are currently under way.

Experimental Section

General Methods. Melting points (uncorrected) were determined on a Thomas-Hoover apparatus. Analytical thin-layer chromatography (TLC) was performed on Merck silica gel F-254 glass-backed plates. Flash chromatography was done as previously described,[50] with use of Woelm 32–63-μm silica gel.

Proton nuclear magnetic resonance (^{1}H NMR) spectra were obtained on a Varian EM-390 (90 MHz), a Varian XL-200 (200 MHz), or a Nicolet Nt-360 (360 MHz) spectrometer; chemical shifts are reported downfield from a tetramethylsilane internal standard (δ scale). Infrared (IR) spectra were obtained on a Perkin-Elmer 137, 1320, or a Nicolet 700 spectrometer in the indicated phase: prominent and diagnostic peaks are reported. Ultraviolet (UV) spectra were determined with a Hewlett-Packard 845A spectrophotometer. Low-resolution mass spectra (MS) were done in the electron-impact mode on the Varian CH-5 spectrometer. The reported data are for an electron energy of 70 eV and follows the form of m/z (intensity relative to base peak = 100). High-resolution mass spectra (HRMS) were obtained in the electron-impact mode on a Varian MAT-371 spectrometer. Analytical gas chromatography (GC) was performed isothermally at 270 °C on a Hewlett-Packard 5790A instrument, with an Alltech RSL-150 capillary column. The corrected fluorescence emission spectra were acquired on a Spex Fluorolog III. For quantum yield determinations, coumarin 311 was used as a standard,[51] and the calculations were done as previously described.[52] Elemental analyses were performed by the Microanalytical Service Laboratory of the University of Illinois.

Molecular mechanics calculations were done with the MAXIMIN option of the SYBYL molecular modeling system (Tripos Associates, St. Louis, MO). Molecular superpositions were also performed with this system, by using the FIT command. Crystallographic coordinates were inputted directly or were obtained from the Cambridge Structural Database via SYBYL.

Unless otherwise noted, a standard procedure for product isolation was used; this involved quenching by addition of water or an aqueous solution, exhaustive extraction with an organic solvent, washing the extracts, drying with $MgSO_4$, and solvent evaporation under reduced pressure. The quenching media, extraction solvents, and aqueous washes used are noted parenthetically after the phrase "product isolation."

Photochemical Methods. Degassing was performed by passing a stream of dry nitrogen through the refluxing solvent for 1 h. Photolyses were carried out in a quartz vessel in Rayonet apparatus, equipped with 14 8-W GE G8T5 254-nm lamps.

X-ray Crystallography. Crystals of **7b** were grown by slow evaporation at 25 °C. Crystals of **10a** were obtained by recrystallization at −30 °C. Diffraction experiments were performed at room temperature with Mo radiation ($\lambda(K_\alpha^-)$ = 0.710 73 Å). Final cell dimensions were obtained by a least-squares fit to the automatically centered settings for at least 15 reflections. Three reference reflections monitored during each experiment showed no significant variation. Intensity data were corrected for Lorentz–polarization effects. Crystal data for both compounds are listed in Table VII. Systematic conditions unambiguously determined the space group for **7b**. The average values and probability distribution of the normalized structure factors for compound **10a** suggested a centric space group; this choice was confirmed by successful refinement.

Both structures were solved by direct methods (MULTAN[53]); correct positions for non-hydrogen atoms were deduced from *E* maps. For both compounds, difference Fourier electron density maps revealed positions for all hydrogen atoms, and the final least-squares refinement cycle (SHELX[54]) included independent parameters for all positions, anisotropic thermal coefficients for non-hydrogen atoms, and a group isotropic thermal parameter

Table VII. Crystal Data for **7b** and **10a**

	7b	**10a**
formula	$C_{24}H_{22}O_3$	$C_{22}H_{16}O_2$
crystal system	monoclinic	triclinic
space group	$P2_1/c$	$P\bar{1}$
a, Å	6.373 (2)	9.734 (5)
b, Å	14.191 (3)	10.512 (3)
c, Å	20.898 (4)	8.922 (4)
α, deg	90	107.02 (3)
β, deg	96.97 (2)	113.96 (4)
γ, deg	90	83.42 (3)
V, Å^3	1876.1 (7)	798 (1)
Z	4	2
density calcd, g/cm^3	1.269	1.300
crystallizing solvent	acetone	methanol
crystal habit	platy (colorless)	columnar (red)
crystal dimensions, mm	0.1 × 0.6 × 0.6	0.2 × 0.2 × 0.6
diffractometer	Syntex $P2_1$	Enraf-Nonius CAD4
μ, cm^{-1}	0.77	0.77
transmission factor range	0.991–0.957 (numerical)	not applied
extinction	not applied	5 (1) × 10^{-7}
2θ limit, deg (octants)	53.0 ($\pm h+k+l$)	52.0 ($+h\pm k\pm l$)
intensities (unique, R_i)	4307 (3633, 0.016)	3389 (3118, 0.013)
intensities > $2.58\sigma(I)$	1855	1910
R	0.046	0.039
R_w (for $w = 1/\sigma^2(F_o) + pF_o^2$)	0.047 (p = 0.016)	0.044 (p = 0.020)
max density in ΔF map, e/Å^3	0.16	0.17

(48) The antiaromatic character of the indenones is manifest in the chemical instability of less substituted indenones. See ref 17.
(49) Katzenellenbogen, J. A.; Carlson, K. E.; Katzenellenbogen, B. S. *J. Steroid Biochem.* **1985**, *22*, 589.
(50) Still, W. C.; Kahn, M.; Mitra, A. *J. Org. Chem.* **1978**, *43*, 2923.
(51) Olmsted, J., III. *J. Phys. Chem.* **1979**, *83*, 2581.
(52) Pesce, A. J.; Rosen, C.-F.; Pasby, T. L. *Fluorescence Spectroscopy*; Marcel Dekker: New York, 1971; pp 177–178.
(53) Main, P.; Fiske, S. J.; Hull, S. E.; Lessinger, L.; Germain, G.; Declercq, J.-P.; Woolfson, M. M. MULTAN 80, a system of computer programs for the automatic solution of crystal structures from X-ray diffraction data, University of York, York, England, 1980.
(54) Sheldrick, G. M. SHELX-76, a program for crystal structure determination, University Chemical Laboratory, Cambridge, England, 1976.

was varied for compound **10a**.[55] For both experiments, the final difference Fourier map had no significant features. Atomic scattering factors and mass attenuation coefficients were taken from *International Tables for X-ray Crystallography*.[56]

1,2-Bis(4-methoxyphenyl)-3-(3-methoxyphenyl)-1-propanone (6b). Sodium hydride (1.06 g, 22.1 mmol) was rinsed with hexane and suspended in THF (5 mL). Desoxyanisoin (**5b**, 4.00 g, 15.6 mmol), dissolved in THF (40 mL), was added dropwise over 2 h. After 4 h at room temperature, the solution was transferred via cannula to a solution of 3-methoxybenzyl chloride (4.96 g, 31.7 mmol) in THF (6 mL). The reaction solution was stirred at room temperature for 40 h. After product isolation (5% HCl, EtOAc, brine), the residue was recrystallized from hexane–THF at −33 °C to afford a white solid (5.24 g, 89%): mp 117–118 °C; IR ($CHCl_3$) 3008, 1670, 1510, 1260 cm^{-1}; ^1H NMR ($CDCl_3$) δ 7.86 (d, 2 H, J = 9 Hz, Ar *H* ortho to CO), 7.23–6.60 (m, 10 H, Ar *H*), 4.70 (t, 1 H, J = 7 Hz, C*H*CO), 3.83 (s, 3 H, OCH_3), 3.73 (s, 3 H, OCH_3), 3.53 (dd, 1 H, J = 15.8 Hz, CH_2), 2.97 (dd, 1 H, J = 15, 8 Hz, CH_2); MS, m/z 376 (10, M^+), 241 (24), 227 (2), 165 (3), 135 (100), 121 (8). Anal. ($C_{24}H_{24}O_4$) C, H.

1,2-Diphenyl-3-(3-methoxyphenyl)-1-propanone (6a). This compound was prepared from deoxybenzoin (**5a**) as described for **6b**. Purification was achieved by flash chromatography (9:1 hexane–acetone), followed by recrystallization (pentane, −78 °C). Yields of **6a**, a white solid, averaged about 69%: mp 60.5–62.5 °C (lit.[7] mp 60.5–62 °C); IR ($CHCl_3$) 3099, 1680, 1490, 1260, 1210 cm^{-1}; ^1H NMR ($CDCl_3$) δ 7.90 (dd, 2 H, J = 6, 1.5 Hz, Ar *H* ortho to CO), 7.48–6.98 (m, 10 H, Ar *H*), 6.75–6.54 (m, 2 H, Ar *H* ortho to OCH_3), 4.55 (t, 1 H, J = 7 Hz, C*H*(Ph)), 3.73 (s, 3 H, OCH_3), 3.68 (dd, 1 H, J = 12, 6 Hz, CH_2), 3.05 (dd, 1 H, J = 12, 6 Hz, CH_2); MS, m/z 316 (6, M^+), 211 (8), 178 (3), 165 (3), 152 (2), 121 (5), 105 (100). Anal. ($C_{22}H_{20}O_2$) C, H.

2,3-Diphenyl-6-methoxyindene (7a). Ketone **6a** (1.10 g) was mixed with 18 g of polyphosphoric acid and stirred mechanically at 40 °C for 6.5 h. Product isolation (ice water, ether, saturated $NaHCO_3$), followed by recrystallization from EtOAc at −30 °C gave 753 mg (73%) of white flakes: mp 130–132 °C (lit.[7] mp 129–131 °C); IR ($CHCl_3$) 3005, 1598, 1475, 1230 cm^{-1}; ^1H NMR (acetone-d_6) δ 7.33–6.73 (m, 13 H, Ar *H*), 3.86 (s, 2 H, CH_2), 3.80 (s, 3 H, -OCH_3); UV (EtOH) λ_{max} 236 (ϵ 28 200), 316 (22 500) nm; fluorescence (EtOH) λ_{em} 426 nm (excitation at 316 nm); MS, m/z 298 (100, M^+), 283 (1), 267 (9), 252 (10), 149 (30). Anal. ($C_{22}H_{18}O$) C, H.

2,3-Bis(4-methoxyphenyl)-6-methoxyindene (7b). This compound was prepared from **6b** in a manner similar to **7a**. The product, a light pink solid, was recrystallized twice from hexane–EtOAc at −33 °C (68%): mp 124.8–125.5 °C; IR ($CHCl_3$) 3000, 2820, 1610, 1580, 1515, 1505, 1250 cm^{-1}; ^1H NMR (DMSO-d_6) δ 7.3–6.7 (m, 11 H, Ar *H*), 3.70 (s, 2 H, CH_2), 3.80 (s, 3 H, OCH_3), 3.77 (s, 3 H, OCH_3), 3.70 (s, 3 H, OCH_3); UV (EtOH) λ_{max} 255 (ϵ 18 800), 315 (24 000) nm; MS, m/z 358 (100, M^+), 343 (6), 327 (5), 315 (7), 300 (2), 284 (3), 269 (3), 239 (6), 227 (4). Anal. ($C_{24}H_{22}O_3$) C, H.

2,3-Diphenyl-6-hydroxyindene (3a). Methoxyindene **7a** (250 mg, 1.17 mmol) was dissolved in 10 mL CH_2Cl_2. $BF_3{\cdot}(CH_3)_2S$ complex (0.5 mL) was added via syringe. After 21 h at room temperature, product isolation (ice water, CH_2Cl_2, 1 M $NaHCO_3$) commenced. The product was purified by flash chromatography (6:1:1 hexane–THF–acetone), followed by recrystallization from hexane–acetone at −30 °C. A straw-colored powder was obtained (168 mg, 50%): mp 113–116 °C; IR (KBr) 3420, 1595, 1458, 1222 cm^{-1}; ^1H NMR ($CDCl_3$) δ 7.3–6.5 (m, 13 H, Ar *H*), 4.76 (s, 1 H, D_2O exch, Ar O*H*), 3.75 (s, 2 H, CH_2); MS, m/z 284 (100, M^+), 267 (5), 265 (8), 252 (9), 239 (7), 226 (3), 207 (14); HRMS calcd/found ($C_{21}H_{16}O$) 284.1201/284.1205.

2,3-Bis(4-hydroxyphenyl)-6-hydroxyindene (3b). Trimethoxyindene **7b** (230 mg, 0.642 mmol) was dissolved in CH_2Cl_2 (10 mL) and cooled to −78 °C. Neat BBr_3 (4.85 mmol) was added via syringe over 2 min. The solution was stirred at −78 °C for 30 min, and the temperature was raised to 0 °C. The reaction was followed by TLC (1:1 hexane–EtOAc) until only a single blue fluorescent spot (R_f 0.30) was evident (16 h). Thereupon the solution was cooled to −78 °C and charged with a solution of triethylamine (1.8 mL) in MeOH (15 mL). The solvent was removed in vacuo, and the product was isolated (water, EtOAc, brine). The residue was purified by flash chromatography (1:1 hexane–EtOAc), followed by two crystallizations from ether–hexane. The product was an amorphous tan solid (68 mg, 34%): mp 179 °C dec; IR (Nujol), 3275, 1610, 1495 cm^{-1}; ^1H NMR (acetone-d_6) δ 8.26 (br s, 3 H, D_2O exch, ArO*H*), 7.43–6.62 (m, 11 H, Ar *H*), 3.75 (s, 2 H, CH_2); MS, m/z 316 (100, M^+), 299 (10), 287 (3), 239 (3), 223 (14), 194 (5), 165 (5), 158 (8); HRMS calcd/found ($C_{21}H_{16}O_3$) 316.109 95/316.1085.

4-Nitrophenyl 3-Methoxybenzoate (8). 3-Methoxybenzoic acid (1.5 g, 9.66 mmol) and 4-nitrophenol (1.44 g, 10.36 mmol) were dissolved in CH_2Cl_2 (20 mL), and dicyclohexylcarbodiimide (2.14 g, 10.36 mmol), dissolved in CH_2Cl_2 (10 mL), was added to the mixture. The solvent was evaporated, and the crude product was eluted through silica with 4:1:1 hexane–EtOAc–$CHCl_3$. Evaporation afforded 2.33 g (86%) of **8** as an off-white powder. An analytical sample was obtained by recrystallization from ether: mp 111–113 °C; IR ($CHCl_3$) 3010, 1745, 1595, 1530, 1490, 1350, 1280, 870 cm^{-1}; ^1H NMR ($CDCl_3$) δ 8.35 (d, 2 H, J = 9 Hz, Ar *H* ortho to NO_2), 7.82 (d, 1 H, J = 7.6 Hz, Ar *H* para to OCH_3), 7.69 (s, 1 H, Ar *H* ortho to CO, and to OCH_3), 7.42 (d, 2 H, J = 9 Hz, Ar *H* meta to NO_2), 7.40 (d? (obscured by previous signal), 1 H, Ar *H* para to CO), 7.25–7.15 (m, 1 H, Ar *H* meta to OCH_3, CO), 3.90 (s, 3 H, OCH_3); MS, m/z 273 (2, M^+), 135 (100), 107 (29); HRMS calcd/found ($C_{14}H_{11}NO_5$) 273.0637/273.0637.

1-(3-Methoxyphenyl)-2,3-bis(4-methoxyphenyl)-1,3-propanedione (9b). Sodium hydride (351 mg, 7.3 mmol) was rinsed with hexane and suspended in THF (5 mL). Desoxyanisoin (**5b**, 750 mg, 2.93 mmol), dissolved in THF (20 mL), was added dropwise over 45 min. After 6 h at 25 °C, ester **8** (800 mg, 2.93 mmol) was added. After 10 h at 25 °C, product isolation (0.5 M HCl, EtOAc, 10% $NaHCO_3$) commenced. A yellowish solid (389 mg, 34%) was obtained. An analytical sample was obtained by recrystallization from hexane–EtOAc: mp 50–53 °C; IR ($CHCl_3$) 3010, 1690, 1665, 1598, 1510, 1250 cm^{-1}; ^1H NMR ($CDCl_3$) δ 7.96 (d, 2 H, J = 9 Hz, Ar *H* meta to OCH_3 of CO-4-MeOAr), 7.55–7.51 (m, 1 H, Ar *H* ortho to OCH_3 and to CO-3-MeOAr; 1 H, Ar *H* para to OCH_3 of 3-MeOAr), 7.36–7.25 (m, 1 H, Ar *H* ortho to OCH_3 and para to CO of 3-MeOAr; 2 H, Ar *H* ortho to CH), 7.08 (dd, 1 H, J = 8, 1 Hz, Ar *H* meta to OCH_3 of 3-MeOAr), 6.90 (d, 4 H, Ar *H* meta to OCH_3 of 4-MeO), 3.84 (s, 3 H, OCH_3 of CO-4-MeOAr) 3.79 (s, 6 H, OCH_3); MS, m/z 390 (10, M^+), 282 (4), 227 (3), 136 (9), 135 (100), 107 (8); HRMS calcd/found ($C_{24}H_{22}O_5$) 390.14673/390.14769.

1-(3-Methoxyphenyl)-2,3-diphenyl-1,3-propanedione (9a). This compound was prepared from **5a** and **8** as described for **9b**. Purification was achieved by flash chromatography of the residue (two runs: 4:1 hexane–acetone; 4:1 hexane–THF), followed by recrystallization from Et_2O at −30 C. The product **9a** was isolated as fine, white needles (33%): mp 112–114 °C; IR ($CHCl_3$) 3000, 2835, 1700, 1675, 1595 cm^{-1}; ^1H NMR ($CDCl_3$) δ 8.1–7.9 (m, 2 H, Ar *H*), 7.55–6.95 (m, 12 H, Ar *H*), 6.55 (s, 1 H, C*H*), 3.80 (s, 3 H, OCH_3); MS, m/z 330 (10, M^+), 135 (100), 105 (89). Anal. ($C_{22}H_{18}O_3$) C, H.

2,3-Diphenyl-6-methoxyindenone 10a by Cyclization of 9a in PPA. Diketone **9a** (160 mg) was mixed with 2.9 g of PPA. The reaction mixture was stirred mechanically at 35 °C for 36 h. Product isolation (ice water, EtOAc, saturated $NaHCO_3$) and recrystallization (19:1 hexane–EtOAc, −25 °C) gave two solids, one in the form of dense dark red prisms, the other a light, amorphous orange solid. A small amount (ca. 2 mg) of the orange solid was separated manually. The remaining crystal mixture was treated with EtOAc in small portions with vigorous agitation. This resulted in fairly selective dissolution of the orange solid, leaving the dark red prisms (94 mg, 62%): mp 159–161 °C; IR ($CHCl_3$) 3000, 1700, 1600, 1475, 1280 cm^{-1}; ^1H NMR ($CDCl_3$) δ 7.48–7.20 (m, 11 H, Ar *H*), 7.04 (d, 1 H, J = 7.9 Hz, Ar *H* ortho to OCH_3 and to CO), 6.80 (dd, 1 H, J = 7.9, 2.5 Hz, Ar *H* ortho to OCH_3, para to CO), 3.86 (s, 3 H, OCH_3); UV (EtOH) λ_{max} 206 (ϵ 32 100) 280 (28 600), 484 (1600) nm; fluorescence (EtOH) none observed for excitation at 488, 300, 270 nm; MS, m/z 312 (100, M^+), 297

(55) Zachariasen, W. H. *Acta Crystallogr.* **1963**, *16*, 1139; *Acta Crystallogr., Sect. A: Cryst. Phys., Diffr., Theor. Gen. Crystallogr.* **1968**, *A24*, 212.

(56) *International Tables for X-Ray Crystallography*; Ibers, J. A., Hamilton, W. C., Eds.; Kynoch: Birmingham, England, 1974; Vol. IV.

(36), 281 (11), 269 (11), 252 (10), 241 (12), 239 (29), 237 (3), 226 (4), 149 (5). Anal. ($C_{22}H_{16}O_2$) C, H.

2,3-Diphenyl-4-methoxyindenone (11). The orange solid isolated in the previous procedure was identified as 11 on the basis of the following characteristics: mp 179–181 °C; IR ($CHCl_3$) 3020, 1700, 1610, 1475, 1270 cm^{-1}; ^1H NMR ($CDCl_3$) δ 7.35–7.10 (m, 12 H, Ar *H*), 6.96 (dd, 1 H, *J* = 6.3, 3.2 Hz, Ar *H* ortho to OCH_3), 3.59 (s, 3 H, OCH_3); MS, *m/z* 312 (100, M^+), 297 (30), 281 (28), 268 (18), 252 (24), 239 (27), 237 (6), 226 (6), 213 (6). HRMS calcd/found ($C_{22}H_{16}O_2$) 312.1158/312.1154.

2,3-Diphenyl-6-methoxyindenone (10a) by Cyclization of 9a in $MeSO_3H$. Diketone **9a** (100 mg, 0.303 mmol) was dissolved in CH_2Cl_2 (10 mL). $MeSO_3H$ (1 mL), dissolved in 10 mL of CH_2Cl_2, was added dropwise over 75 min. The reaction solution was stirred at 25 °C for 25 h. After preliminary product isolation (ice water, partition of phases), the CH_2Cl_2 layer was subjected to GC analysis. A 9:1 ratio of the para isomer **10a** to the ortho isomer (**11**) was observed. Evaporation of the organic layer and recrystallization from MeOH at −30 °C afforded 63 mg (62%) of **10a**, identical with that obtained by PPA cyclization. This reaction was also conducted at 0 °C; the ratio of **10a**/**11** increased to 16.4:1 with 80% of **10a** isolated. No reaction occurred at −33 °C.

2,3-Diphenyl-6-methoxyindenone (10a) by SeO_2 Oxidation. Monomethoxyindene **7a** (139 mg 0.466 mmol) and SeO_2 (104 mg, 0.937 mmol) were dissolved in 95% EtOH (10 mL). The solution was heated at reflux for 78 h, after which the Se metal was removed by filtration, and the filtrate was evaporated. Product isolation (water, ether, 1 M $NaHCO_3$), followed by flash chromatography (two runs: 4:1 hexane–acetone; 9:1 hexane–EtOAc) and recrystallization (9:1 hexane–EtOAc, −25 °C) gave a dark red amorphous solid (74 mg, 51%) identical with that obtained by cyclization of diketone **9a**.

2,3-Bis(4-methoxyphenyl)-6-methoxyindenone (10b) by Cyclization of 9b in $MeSO_3H$. This compound was prepared from diketone **9b** in a manner similar to **10a**, except a longer reaction time was required (5.5 days, 25 °C). Product isolation (ice water, CH_2Cl_2, saturated $NaHCO_3$), followed by flash chromatography (9:1 hexane–THF) afforded 189 mg of **10b** (67%) as a dark red solid. There was apparently none of the other possible regioisomer. An analytical sample was obtained by recrystallization from MeOH at 25 °C: mp 113–115 °C; IR ($CHCl_3$) 3010, 1700, 1610, 1515, 1505, 1480, 1250 cm^{-1}; ^1H NMR ($CDCl_3$) δ 7.34 (d, 2 H, *J* = 9 Hz, Ar *H* meta to OCH_3 on 3-Ar), 7.20 (d, 2 H, *J* = 9 Hz, Ar *H* meta to OCH_3 on 2-Ar), 7.16 (d, 1 H, *J* = 3 Hz, Ar *H* on C-7), 7.06 (d, 1 H, *J* = 8 Hz, Ar *H* on C-4), 6.92 (d, 2 H, *J* = 9 Hz, Ar *H* ortho to OCH_3 on 3-Ar), 6.80 (d, 2 H, *J* = 9 Hz, Ar *H* ortho to OCH_3 on 2-Ar), 6.80–6.75 (m, 1 H, Ar *H* on C-5), 3.85 (s, 6 H, OCH_3 of 2-Ar and 3-Ar), 3.79 (s, 3 H, OCH_3 on C-6); MS, *m/z* 372 (100, M^+), 357 (41), 341 (4), 329 (5), 314 (4), 298 (5), 271 (4), 255 (4), 243 (6), 226 (6), 215 (7), 186 (9), 135 (31). Anal. ($C_{24}H_{20}O_4$) C, H.

2,3-Bis(4-methoxyphenyl)-6-methoxyindenone (10b) by SeO_2 Oxidation. Inexplicably, direct oxidation of trimethoxyindene **7b** proved more difficult than for methoxyindene **7a**. SeO_2, with or without added *t*-BuOOH (1–20 equiv),[57] gave only 13–23% of the desired indenone.

2,3-Diphenyl-6-hydroxyindenone (4a). Methoxyindenone **10a** (150 mg, 0.48 mmol) and dry pyridine hydrochloride (5.8 g) were heated to 160 °C for 24 h. Production isolation (5% HCl, EtOAc, saturated $CuSO_4$), followed by flash chromatography (4:1 hexane–EtOAc), gave 136 mg (95%) of **4a** as a dark red solid. An analytical sample was provided by recrystallization from hexane–ethyl acetate at −30 °C: mp 177.3–177.9 °C; IR (CH_2Cl_2) 3560, 1700, 1610, 1365 cm^{-1}; ^1H NMR ($CDCl_3$) δ 7.45–7.32 (m, 4 H, Ar *H*), 7.29–7.19 (m, 7 H, Ar *H*), 6.77 (dd, 1 H, *J* = 7.9, 2.2 Hz, Ar *H* ortho to OH, para to CO), 5.15 (s, 1 H, D_2O exch, Ar O*H*); MS, *m/z* 298 (100, M^+), 281 (16), 269 (9), 252 (8), 239 (23), 213 (4). Anal. ($C_{21}H_{14}O_2$) C, H.

2,3-Bis(4-hydroxyphenyl)-6-hydroxyindenone (4b). This compound was prepared from trimethoxyindenone **10b** as described for **4a**. Purification was achieved by recrystallization from hexane–EtOAc at −30 °C. A dark purple-red powder was obtained (75%): mp 274.5–276.5 °C; ^1H NMR (acetone-d_6) δ 8.76 (br s, Ar O*H*), 7.29 (d, 2 H, *J* = 9 Hz, Ar *H* meta to OH on 3-Ar), 7.10 (d, 2 H, *J* = 9 Hz, Ar *H* meta to OH on 2-Ar), 7.05 (d, 1 H, *J* = 9 Hz, Ar *H* on C-4), 6.99 (d, 1 H, *J* = 2 Hz, Ar *H* on C-7), 6.91 (d, 2 H, *J* = 9 Hz, Ar *H* ortho to OH on 3-Ar), 6.82 (dd, 1 H, *J* = 9, 3 Hz, Ar *H* on C-5), 6.74 (d, 2 H, *J* = 9 Hz, Ar *H* ortho to OH on 2-Ar); MS, *m/z* 330 (100, M^+), 313 (21), 301 (6), 284 (5), 273 (7), 255 (11), 226 (7), 189 (5), 165 (7), 151 (7), 113 (11); HRMS calcd/found ($C_{21}H_{14}O_4$) 330.0892/330.0893.

Irradiation of 7a (under Conditions of Trial 5 in Table IV). Indene **7a** (100 mg, 0.355 mmol) was dissolved in 17 mL of cyclohexane. The solution was irradiated at 254 nm for 4 h. The solvent was evaporated, and the residue was subjected to flash chromatography (9:1 pentane–THF). Three compounds were isolated in order of increasing column retention:

6-Methoxyindene[2,3-*g*]phenanthrene (17). This compound was separated from an uncharacterized red product by repeated crystallization from ether at −78 °C to give 5 mg (5%) of an off-white solid: mp 160–163 °C; ^1H NMR (CCl_4) δ 8.71–8.58 (m, 3 H, bay region Ar *H*, *peri* Ar *H* away from CH_2), 8.15 (d, 1 H, *J* = 9 Hz, *peri* Ar *H* near CH_2), 7.93–7.91 (m, 1 H, phenanthrene Ar *H*), 7.65–7.61 (m, 3 H, Ar *H*), 7.53–7.44 (m, 2 H, Ar *H*), 6.87 (dd, 1 H, *J* = 9, 2 Hz, Ar *H* ortho to OCH_3, meta and para to 5-ring), 4.11 (s, 2 H, CH_2), 3.86 (s, 3 H, OCH_3); UV (EtOH) λ_{max} 208 (ϵ 58 600), 248 (49 600), 264 (44 700), 328 (19 400) nm; fluorescence (EtOH) λ_{em} 398 nm (excitation at 328 nm); MS, *m/z* 296 (100, M^+), 281 (48), 253 (22), 226 (3), 148 (17, M^{2+}); HRMS, calcd/found ($C_{22}H_{16}O$) 296.1201/296.1114.

2-Benzoyl-5-methoxybenzoic Acid (19). Evaporation of the fractions that showed a weak yellow fluorescence under longwave UV on TLC (R_f 0.2, 9:1 pentane–THF) gave a yellow oil (9.7 mg, 11%): IR (neat) 2990, 1750, 1690, 1610, 1105, 879, 740 cm^{-1}; MS, *m/z* 256 (4, M^+), 239 (4), 227 (2), 212 (2), 196 (3), 135 (5), 105 (100); HRMS, calcd/found ($C_{15}H_{12}O_4$) 256.0735/256.0733, calcd/found (C_7H_5O) 105.0340/105.0340.

1-Oxo-6-methoxyindeno[2,3-*g*]phenanthrene (18). Evaporation of fractions showing a red spot on TLC (R_f 0.17, 9:1 pentane–THF) afforded a red solid (19 mg, 18%): mp 219–221 °C; IR (thin film) 3050, 1650, 1605, 1210 cm^{-1}; ^1H NMR (DMSO-d_6) δ 9.06 (d, 1 H, *J* = 8.1 Hz, *peri* Ar *H* near CO), 8.97 (d, 1 H, *J* = 8.3 Hz, bay region Ar *H* near CO), 8.85 (d, 1 H, *J* = 8.1 Hz, other *peri* Ar *H*), 8.79 (d, 1 H, *J* = 8.4 Hz, other bay region Ar *H*), 7.76–7.52 (m, 2 H, Ar *H*), 7.19 (d, 1 H, *J* = 2.4 Hz, Ar *H* ortho to OCH_3, ortho to OC), 7.10 (dd, 1 H, *J* = 8.2, 2.4 Hz, Ar *H*, ortho to OCH_3, para to CO), 3.97 (s, 3 H, OCH_3); MS, *m/z* 310 (100, M^+), 295 (38), 267 (12), 239 (37), 155 (12, M^{2+}); HRMS calcd/found ($C_{22}H_{14}O_2$) 310.1000/310.0997.

6-Hydroxyindeno[2,3-*g*]phenanthrene (20). Hydroxyindene **3a** (105 mg, 0.37 mmol) was dissolved in 5:1 cyclohexane–THF (30 mL). I_2 (6 mg) was added. The solution was irradiated with 15 254-nm lamps under an N_2 atmosphere for 10.5 h. The solvent was evaporated, and the residue was suspended in EtOAc and washed with 0.1 M $Na_2S_2O_3$. The organic layer was dried ($MgSO_4$), evaporated, and twice subjected to flash chromatography (6:1:1 pentane–EtOAc–THF; benzene). Evaporation of the appropriate fractions, followed by crystallization from THF–hexane, provided 4.5 mg (4%) of a light tan solid: mp 210 °C dec; ^1H NMR ($CDCl_3$) δ 8.97–8.80 (m, 3 H, Ar *H*), 8.60 (s, 1 H, D_2O exch, Ar O*H*), 8.35 (d, 1 H, *J* = 8.6 Hz, Ar *H*), 8.18 (d, 1 H, J = 8.6 Hz, Ar *H*), 7.85–7.62 (*m*, 5 H, Ar *H*), 7.05 (d, 1 H, *J* = 8.6 Hz, Ar *H*), 4.29 (s, 2 H, CH_2); MS, 282 (100, M^+), 265 (1), 252 (22), 250 (10), 226 (3), 141 (12, M^{2+}); HRMS, calcd/found ($C_{21}H_{14}O$) 282.1045/282.1041.

Acknowledgment. We are grateful for support of this research through a grant from the National Institutes of Health (PHS 5R01 DK 15556). High-field NMR spectra and high-resolution mass spectra were obtained on instruments supported by grants from the National Institutes of Health (RR 02299 and GM 27029, respectively). We are thankful to Kathryn E. Carlson for performing the estrogen receptor binding assays.

Registry No. **2**, 103088-13-7; **3a**, 114095-29-3; **3b**, 114095-39-5; **4a**, 79612-08-1; **4b**, 114095-35-1; **5a**, 451-40-1; **5b**, 120-44-5; **6a**, 53347-52-7; **6b**, 114095-36-2; **7a**, 53347-55-0; **7b**, 95956-56-2; **8**, 36718-85-1; **9a**, 114095-85-1; **9b**, 114095-37-3; **10a**, 70603-19-9; **10b**,

(57) Umbreit, M. A.; Sharpless, K. B. *J. Am. Chem. Soc.* **1977**, *99*, 5526.

114095-38-4; 11, 70603-18-8; 12, 586-38-9; 13, 10540-29-1; 14, 1845-11-0; 15, 114095-31-7; 17, 114095-32-8; 18, 114095-33-9; 19, 2159-48-0; 20, 114095-34-0; 3-methoxybenzyl chloride, 824-98-6; 4-nitrophenol, 100-02-7.

Supplementary Material Available: Atomic numbering schemes, tables of atomic coordinates, thermal parameters, bond lengths, and bond angles for compounds 7b and 10a (10 pages). Ordering information is given on any current masthead page.

Methotrexate Analogues. 32. Chain Extension, α-Carboxyl Deletion, and γ-Carboxyl Replacement by Sulfonate and Phosphonate: Effect on Enzyme Binding and Cell-Growth Inhibition[1]

Andre Rosowsky,*† Ronald A. Forsch,† Richard G. Moran,‡ William Kohler,§ and James H. Freisheim§

Dana-Farber Cancer Institute and Department of Pharmacology, Harvard Medical School, Boston, Massachusetts 02115, Division of Hematology/Oncology, Children's Hospital of Los Angeles, Los Angeles, California 90027, and Department of Biochemistry, Medical College of Ohio, Toledo, Ohio 43699. *Received September 3, 1987*

Analogues of methotrexate (MTX) and aminopterin (AMT) with aminophosphonoalkanoic, aminoalkanesulfonic, and aminoalkanephosphonic acid side chains in place of glutamate were synthesized and tested as inhibitors of folylpolyglutamate synthetase (FPGS) from mouse liver. The aminophosphonoalkanoic acid analogues were also tested as inhibitors of dihydrofolate reductase (DHFR) from L1210 murine leukemia cells and as inhibitors of the growth of MTX-sensitive (L1210) and MTX-resistant (L1210/R81) cells in culture. The optimal number of CH_2 groups in aminophosphonoalkanoic acid analogues of AMT was found to be two for both enzyme inhibition and cell growth inhibition but was especially critical for activity against FPGS. Deletion of the α-carboxyl also led to diminished anti-FPGS activity in comparison with previously studied homocysteic acid and 2-amino-4-phosphonobutyric acid analogues. In the aminoalkanesulfonic acid analogues of MTX without an α-carboxyl, anti-FPGS activity was low and showed minimal variation as the number of CH_2 groups between the carboxamide and sulfonate moieties was changed from one to four. In similar aminoalkanephosphonic acid analogues of MTX, anti-FPGS activity was also low, was comparable for two and three CH_2 groups between the carboxamide and phosphonate moieties, and was diminished by monoesterification of the phosphonate group. These effects demonstrate that the α-carboxyl group of folate analogues is involved in binding to the active site of FPGS, and that an α-carboxyl group should be retained as part of the structure of FPGS inhibitors.

Folylpolyglutamate synthetase (FPGS) inhibitors are of potential chemotherapeutic interest because of the importance of this enzyme in cellular folate metabolism.[2] Mutant cell lines lacking FPGS are severely impaired in their capacity to utilize reduced folate cofactors for the synthesis of the nucleotide precursors of DNA and, therefore, are auxotrophic for thymidine and purines.[3,4] Selective disruption of reduced folate metabolism by FPGS inhibitors in tumors as opposed to normal tissues has been proposed as a strategy for the development of new antifolates as cancer drugs.[5]

Considerable work has been done over the past several years to elucidate the general structural features that a compound should have in order to be a good FPGS substrate or inhibitor.[6-8] As part of our overall program of systematic modification of the side chain in methotrexate (MTX, 1) and aminopterin (AMT, 2), we have demonstrated that analogues 3–6 are moderately potent inhibitors of FPGS from mouse liver.[9,10] Inhibition of human FPGS by these analogues has also been reported.[11] The sulfonates 3 and 4 were made in both the L and DL configurations, while the phosphonates 5 and 6 were made only in the DL form. The K_i's of 3 and 4 were almost the same as the K_m(app) of MTX, while those of 5 and 6 were comparable to the K_m(app) of AMT.

As part of an ongoing structure–activity study of potential FPGS inhibitors aimed at a more precise delineation of the molecular features that contribute to active-site binding, we were interested in whether (a) the anti-FPGS activity of compounds with a sulfonic or phosphonic acid group on the end of the side chain requires the presence

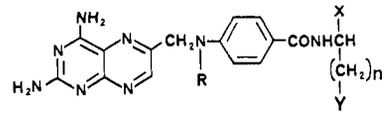

	R	n	X	Y
1 (MTX)	Me	2	COOH	COOH
2 (AMT)	H	2	COOH	COOH
3	Me	2	COOH	SO_2OH
4	H	2	COOH	SO_2OH
5	Me	2	COOH	$PO(OH)_2$
6	H	2	COOH	$PO(OH)_2$
7	H	1	COOH	$PO(OH)_2$
8	H	3	COOH	$PO(OH)_2$
9	H	4	COOH	$PO(OH)_2$
10	Me	0	H	SO_2OH
11	Me	1	H	SO_2OH
12	Me	2	H	SO_2OH
13	Me	3	H	SO_2OH
14	Me	1	H	$PO(OH)_2$
15	Me	2	H	$PO(OH)_2$
16	Me	2	H	PO(OH)(OEt)
25	Me	2	H	$PO(OEt)_2$

† Dana-Farber Cancer Institute.
‡ Children's Hospital of Los Angeles.
§ Medical College of Ohio.

(1) Paper 31 in this series: Rosowsky, A.; Forsch, R. A.; Moran, R. G.; Freischeim, J. H. *J. Med. Chem.*, in press.
(2) For a useful overview of the folylpolyglutamate synthetase field prior to 1983, see: *Folyl and Antifolyl Polyglutamates*; Goldman, I. D., Chabner, B. A., Bertino, J. R., Eds.; Plenum: New York, 1983.
(3) McBurney, M. W.; Whitmore, G. F. *Cell* **1974**, *2*, 173.
(4) Taylor, R. L.; Hanna, M. L. *Arch. Biochem. Biophys.* **1979**, *181*, 331.
(5) Moran, R. G. In *Proceedings of the Second Workshop on Folyl and Antifolyl Polyglutamates*; Goldman, I. D., Ed.; Praeger: New York, 1985; pp 51–64.

0022-2623/88/1831-1326$01.50/0